C. R. Chimie 16 (2013) 201–206

Contents lists available at SciVerse ScienceDirect

Comptes Rendus Chimie

www.sciencedirect.com

Preliminary communication/Communication

Synthesis, characterization, X-ray diffraction, antimicrobial and in vitro cytotoxicity studies of 7a-Aza-B-homostigmast-5-eno [7a,7-d] tetrazole

Mahboob Alam [a], Shahab A.A. Nami [b,c,*], Ahmad Husain [d], Dong-Ung Lee [a], Soonheum Park [b]

[a] Division of Bioscience, Dongguk University, Gyeongju 780-714, Republic of Korea
[b] Department of Chemistry, Dongguk University, Gyeongju 780-714, Republic of Korea
[c] Department of Kulliyat, Faculty of Unani Medicine, Aligarh Muslim University, Aligarh 202002, India
[d] Department of Chemistry, Aligarh Muslim University, Aligarh 202002, India

ARTICLE INFO

Article history:
Received 10 July 2012
Accepted after revision 19 December 2012
Available online 19 January 2013

Keywords:
Tetrazole
Hydrazoic acid
Crystal structure
Antimicrobial activity
Cytotoxicity

ABSTRACT

The synthesis, spectral characterization, crystal structure and antimicrobial activity of the novel synthetic molecule 7a-Aza-B-homostigmast-5-eno [7a,7-d] tetrazole, $C_{29}H_{48}N_4$ has been reported. The structure has also been determined by X-ray diffraction technique using direct method and was refined on F^2 by the full-matrix least-squares. Crystals are orthorhombic and their space group is *P212121*, with $a = 7.230(3)$, $b = 31.451(13)$, $c = 11.974(5)$ (Å), $\alpha = \beta = \gamma = 90^\circ$. It can be conveniently obtained by the reaction of 7-Oxostigmast-5-ene with hydrazoic acid. The molecule has also been screened for its possible in vitro antimicrobial activity against *Staphylococcus aureus*, *Streptococcus mutans*, *Streptococcus pyogenes, Staphylococcus epidermidis*, *Bacillus cereus*, *Corynebacterium xerosis, Escherichia coli*, *Klebsiella pneumoniae, Proteus vulgaris* and *Pseudomonas aeruginosa* (MTCC 424). Minimum inhibitory concentration (MIC) of the synthesized compound has also been evaluated. The highest activity is observed against *C. xerosi* and *P. vulgaris*. Moreover, the compound has also been screened for its in vitro cytotoxicity against human colon carcinoma cell line, HCT116 and human liver hepatocellular carcinoma cell line, HepG2, using doxorubicin as standard. On the basis of its IC_{50} values, 7a-Aza-B-homostigmast-5-eno [7a,7-d] tetrazole was found to inhibit the cancer cells effectively.

1. Introduction

Steroids and their derivatives have fascinated not only chemists and biochemists but also endocrinologists because of their ability to penetrate cells and eventually bind to nuclear and membrane receptors [1]. The most potent active endocrine compounds like progesterone, estrogens, androgens, etc., which are responsible for human evolution and perpetuation belong to the chemical class of steroids. Butenandt and Ruzicka have earned the Nobel Prize for chemistry late back in 1935 for the successful synthesis and characterization of testosterone [2,3]. The biological and chemical applications of steroidal derivatives are numerous and are still a vibrant area of research because of the scientific breakthroughs [4]. On the other hand, tetrazoles represent an important class of nitrogen-containing heterocycles, which exhibit a wide spectrum of applications ranging from medicinal to synthetic chemistry [5]. From synthetic viewpoint, tetrazoles are effectively used in the study of receptor–substrate interaction [6], as catalysts [7], propellants [8], explosives [9] and in high-energy chemistry [10]. Tetrazole derivatives are also found to possess robust biological activities like antiviral, antibacterial, anti-allergic, anti-convulsant, anti-inflammatory properties and as carboxylic acids isosteres [11,12]. Furthermore, tetrazole moieties are important synthons in synthetic organic

* Corresponding author.
E-mail addresses: saanami.tc@amu.ac.in, saanami@dongguk.ac.kr (Shahab A.A. Nami).

1631-0748/$ – see front matter
http://dx.doi.org/10.1016/j.crci.2012.12.018

chemistry and are the key starting material for a number of important derivatives [13]. Hence, keeping in view the exciting characteristics of steroids and tetrazoles and in continuation of our quest on steroidal tetrazoles, we herein report the synthesis, X-ray diffraction, antimicrobial and in vitro cytotoxicity studies of 7a-Aza-B-homostigmast-5-eno [7a,7-d] tetrazole starting from 7-Oxostigmast-5-ene.

2. Experimental

2.1. Apparatus and reagents

Melting points were determined on a Kofler apparatus and are uncorrected. IR spectra were recorded as neat with a Pye Unicam SP-3-100-spectrophotometer and their values are given in cm^{-1}. The ^{1}H and ^{13}C NMR spectra were recorded in $CDCl_3$ using JEOL Eclipse (400 and 100 MHz) instrument having tetramethylsilane (TMS) as internal standard and values are given in parts per million (ppm). Elemental analyses (C, H and N) were carried out with a Carlo Erba EA-1108 analyzer. Thin-layer chromatography (TLC) was performed on glass plates precoated with silica gel G and exposed to iodine vapors to monitor the reactions and to certify the purity of the reaction products. Silica gel (mesh size 60–120, BDH) was used for (~25 g for each gram of material) purification using gravity column chromatography. Petroleum ether refers to a fraction of b.p. 60–80 °C. Sodium sulfate (anhydrous) was used as a drying agent for organic extracts after reaction work-up. All the solvents were distilled prior to use. The method of Moural and Syhora [14] was used to prepare a hydrazoic acid solution.

2.2. In vitro cytotoxicity

The in vitro cytotoxicity of 7a-Aza-B-homostigmast-5-eno [7a,7-d] tetrazole was performed employing the cell lines HCT116 (human colon carcinoma cell line), HepG2 (human liver hepatocellular carcinoma cell line) and one non-cancerous HFL1 (human lung fibroblast), using a standard 3-(4,5-dimethyl-thiazol-2-yl)-2,5-diphenyl-tetrazolium bromide (MTT) reduction assay.

Cells in exponential growth were seeded into 96-well plates at a concentration of 5×10^5 cells/200 μL/well and allowed to grow in specific medium containing 5% FCS. After 24 h, cells were treated with various concentrations of test compound in a concentration range of 0–25 μM. Control (dimethyl sulphoxide [DMSO only]) and positive control (doxorubicin, used as a standard drug) cells were cultured using identical conditions. After 4 days (96 h) of incubation, the medium was removed and replaced with fresh medium. MTT reagent (5 mg/mL in PBS) was added to each well at a volume of 1:10 and incubated for 2 to 3 h at 37 °C. After treatment, 100 mL of DMSO were added to each well after carefully aspirating the supernatants. Absorbance was measured at 620 nm in a multi-well plate reader. Triplicate wells were prepared for each individual concentration. Dose-response curves were plotted as percentages of the cell absorbance. Drug sensitivity was expressed in terms of the concentration of drug required for a 50% reduction of cell viability (IC_{50}).

The IC_{50} value was defined as the concentration of test sample resulting in a 50% reduction of absorbance as compared with untreated controls that received a serial dilution of the solvent in which the test samples were dissolved, and was determined by linear regression analysis. Doxorubicin was used as the standard drug throughout.

2.3. Preparation of the steroidal 7a-Aza-B-homostigmast-5-eno [7a,7-d] tetrazole

To a cooled solution of hydrazoic acid in benzene, a freshly distilled borontrifluoride etherate solution (1.5 mL) was added dropwise with continuous stirring maintaining the temperature below 5 °C. To this reaction mixture, a pre-cooled solution of 7-Oxostigmast-5-ene [15] (2 g) in benzene (25 mL) was added over a period of about 5 h with vigorous stirring (Scheme 1).

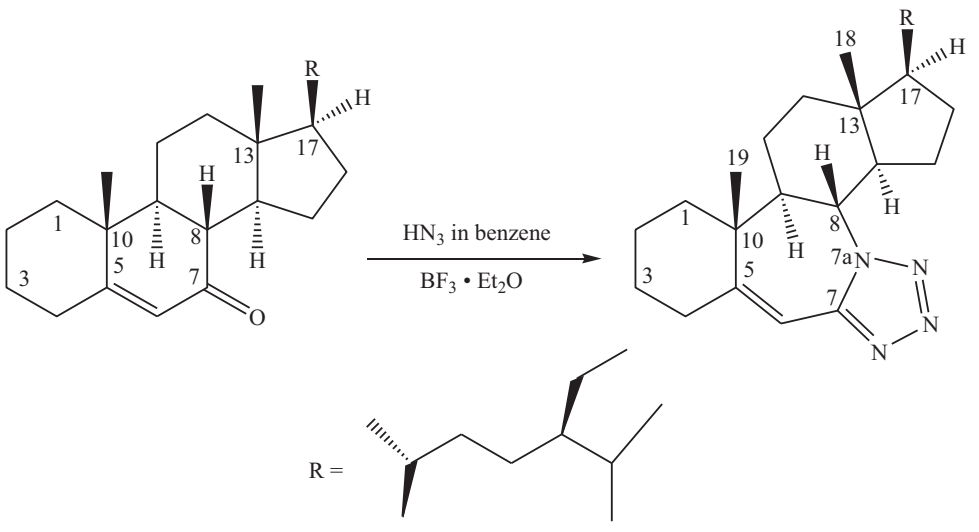

Scheme 1. Synthesis of the title compound.

The reaction mixture was then allowed to stand at room temperature for 30 h. The solution was washed successively with water, sodium bicarbonate solution (5%) and dried over (Na_2SO_4). Benzene was removed under reduced pressure and the residue (2.1 g) was chromatographied over silica gel (40 g) and eluted in 30 mL portions. Elution with benzene–ether (10:1) affords (8.5 g) the title compound. Crystallization was done using light petroleum to obtain transparent rectangular-shaped crystals. (78% yield) M.p. 453 K: FT-IR (KBr, cm^{-1}): 1670 (s, $\nu_{C=C}$), 1505, 1465, 1380 (coupled $\nu_{C=N+N=N}$). ^1H NMR (300 MHz, $CDCl_3$): 6.55, s (C6–H); 4.18, br (C8–βH); 1.23, 1.10, 0.98, s (Methyl protons). Anal. Calc. for $C_{29}H_{48}N_4$ (M_r = 452.72): C, 76.94; H, 10.69; N, 12.37%. Found: C, 76.59; H, 10.49; N, 12.72%.

2.4. Crystal structure determination and refinements

Single crystals suitable for X-ray crystallographic analyses were obtained by slow evaporation of solvent from the chloroform solution at room temperature. A crystal of dimensions 0.05 × 0.05 × 0.20 mm was selected for intensity data and X-ray data was collected using graphite-monochromated Mo Kα radiation (λ = 0.71073 Å) on Bruker SMART APEX CCD Diffractometer at 100 K. The program SMART [16] was used for collecting frames of data, indexing reflections, and determining lattice parameters. The data integration and reduction were processed with SAINT [16]. An empirical absorption correction was applied to the collected reflections with SADABS [17] using XPREP [18]. The linear absorption coefficients, scattering factors for the atoms and the anomalous dispersion corrections were taken from the International Tables for X-ray Crystallography [19]. The structure was solved by the direct method and was refined on F^2 by the full-matrix least-squares technique using the SHELXL97 program [20] package while additional crystallographic calculations were performed by PLATON [21]. Figures were drawn using ORTEP–3.2 [22] and MERCURY–2.4 [23]. All non-hydrogen atoms were refined with anisotropic displacement parameters. Hydrogen atoms were located from the difference Fourier map refined as riding entities. The atomic scattering factors were those included in SHELXL97. The final refinement cycles converged to an $R = 0.0637$ and $R_W(F)^2 = 0.1432$ for the observed data. The pertinent crystal data and refinement parameters are compiled in Table 1.

Table 1
^{13}C NMR spectral data of the compound.

Position of carbon	^{13}C NMR	Position of carbon	^{13}C NMR
1	38.7	16	28.9
2	31.5	17	56.3
3	25.9	18	11.9
4	38.1	19	18.1
5	137.0	20	36.2
6	141.0	21	21.7
7	160.0	22	36.3
8	39.0	23	28.1
9	49.7	24	39.5
10	36.9	25	27.9
11	22.9	26	22.3
12	39.8	27	22.8
13	43.1	28	23.1
14	56.8	29	18.6
15	23.8		

2.5. In vitro antibacterial activity

2.5.1. Test microorganisms and medium

Ten bacterial strains (six Gram positive and four Gram negative) were selected on the basis of their clinical importance in causing diseases in humans. These were obtained from Hi media Labs Pvt. Ltd., Mumbai, India and Microbial Type Culture Collection, Chandigarh, Punjab, India. The strains so selected for the study are *Staphylococcus aureus* (ATCC 29213), *Streptococcus mutans* (ATCC 25175), *Streptococcus pyogenes* (MTCC 435), *Staphylococcus epidermidis* (MTCC 435), *Bacillus cereus* (MTCC 430), *Corynebacterium xerosis* (ATCC 373) (Gram-positive bacterial strains), *Escherichia coli* (ATCC 25922), *Klebsiella pneumoniae* (MTCC 109), *Proteus vulgaris* (MTCC 426) and *Pseudomonas aeruginosa* (MTCC 424). These strains were screened for evaluation of antibacterial activities of the synthesized chemical compounds.

The solid media, namely Nutrient Agar No.2 (NA) (M 1269S-500G, Himedia Labs Pvt. Ltd, Bombay, India), was used for preparing nutrient plates, while Nutrient Broth (NB) (M002-500G, Himedia Labs Pvt. Ltd, Bombay, India) was used for the liquid culture media.

2.5.2. Primary screening

The antibacterial activity of the synthesized compound was evaluated by agar well diffusion method. All the microbial cultures were adjusted to 0.5 McFarland standards, which is visually comparable to a microbial suspension of approximately 1.5×10^8 cfu/mL. Twenty mL of agar media were poured into each Petri plate and plates were swabbed with a colony from the inoculums of the test microorganisms and kept for 15 min for adsorption. Using sterile cork borer of 6 mm diameter, wells were bored into the seeded agar plates and these were loaded with a 50 μL volume with a concentration of 10 mg/mL of each compound reconstituted in the DMSO. All the plates were incubated at 37 °C for 24 h.

Antimicrobial activity of the synthesized compound was evaluated by measuring the zone of growth inhibition against the test microorganisms with Antibiotic Zone Scale (PW297, Himedia Labs Pvt. Ltd., Mumbai, India), which was holded over the back of the inverted plate. The plate was held a few inches above a black, non-reflecting background and illuminated with reflected light. The medium with DMSO as a solvent was used as a negative control whereas media with ciprofloxacin (standard antibiotic for Gram positive) and gentamicin (standard antibiotic for Gram negative) were used as positive controls. The experiments were performed in triplicate.

2.5.3. Determination of minimum inhibitory concentration of synthesized compound

Minimum inhibitory concentration (MIC) is the lowest concentration of an antimicrobial compound that will

inhibit the visible growth of microorganisms after overnight incubation. MICs are important in diagnostic laboratories to confirm resistance of microorganisms to antimicrobial agents and also to monitor the activity of new antimicrobial agents. The MIC of the chemically synthesized compound was tested against bacterial strains through a broth dilution method. In this method, the test concentration of synthesized compounds was made from 2.5 to 0.01 mg/mL in the sterile wells of the microtiter plates.

2.5.4. Broth dilution method

In a sterile microtitre plates (96-u-shaped wells), 50 μL of the sterile nutrient broth were poured in each well in three rows, than from a fresh inoculum so formed (108 cfu/ml diluted with 100 μL nutrient broth to have 106 cfu/mL). 50 μL of the suspension were poured in each well in the first and third rows, the second row was filled with 50 μL of nutrient broth, finally the drug sample 50 μL was added in the first row diluting uniformly from 2.5 to 0.01 mg/mL till the eighth well. MIC was expressed as the lowest dilution which inhibited the growth judged by lack of turbidity in the well. All the microtiter plates were wrapped properly with a sterilized foil and incubated at 37 °C for 18–24 hours.

3. Results and discussion

3.1. Chemistry

The starting compound, 7-Oxostigmast-5-ene, has been synthesized by the literature's method [15] in 68% yield. Its purity has been ascertained on the basis of TLC. Moreover, the precursor has also been subjected to spectral (IR and ^{1}HNMR) and micro-analytical (C, H and N) analysis. The title compound has been synthesized in good yield (please see experimental). The selected diagnostic IR bands of the synthesized compound provide useful information for determining the structure of the tetrazole derivative. The strong absorption band at 1670 cm^{-1} may be assigned to the C=C group while the closely spaced bands observed at 1505, 1465 and 1380 cm^{-1} may be ascribed to the coupling of C=N and N=N groups, implying the formation of the tetrazole derivative [24].

In the ^{1}HNMR spectrum, the assignments of the signals are based on the chemical shift and intensity pattern. The spectrum of the compound 7a-Aza-B-homostigmast-5-eno [7a,7-d] tetrazole exhibited singlets at δ 0.67 and 1.23 for angular methyl groups C–18 and C–19. Three set of doublets are observed at δ 0.98 (J = 6.4 Hz), 0.81 (J = 7 Hz) and 0.79 (J = 7 Hz) for C–21, C–26 and C–27 methyl groups respectively while a triplet was observed at δ 1.10 (J = 4.1 Hz) for C–29 methyl group, ascertaining the proposed structure (Fig. 1). However, the broad band appearing at 4.18 ppm may be regarded as C8–βH. A sharp singlet appearing at 6.55 ppm may be ascribed for C6–H, which is in close proximity with other reports [15]. The methylene and methane protons were found to resonate in the range 1.17–2.39 ppm.

The ^{13}C NMR signals are also in good corroboration with the proposed structure of the title compound. The strong signal at δ 160 shows the presence of the C=N group, while the signal at 137 ppm corresponds to the C=C group of C5 (ring B). However, for C6 the peak shifts a little upfield and was found to resonate at 141 ppm (Scheme 2). The assignments for methyl, methylene and methane carbons are summarised in Table 1.

3.2. In vitro cytotoxicity

The compound 7a-Aza-B-homostigmast-5-eno [7a,7-d] tetrazole was tested against two human cancer cell lines: HCT116 and HepG2 and one non-cancerous HFL1 (human lung fibroblast) cell line. The IC_{50} values for these

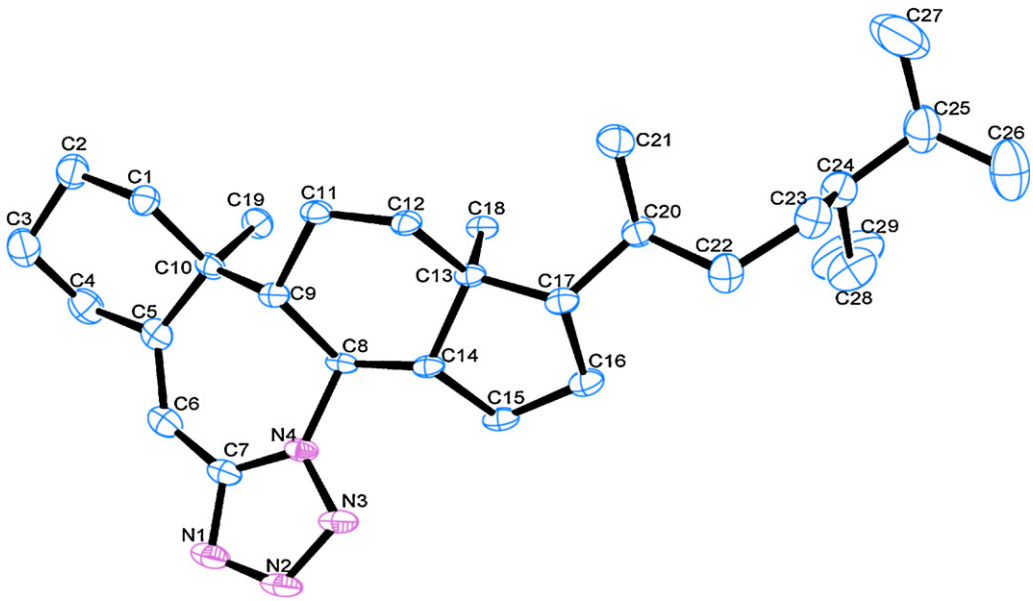

Fig. 1. Ortep view of the molecular structure (showing 30% thermal ellipsoids), along with the atomic numbering scheme. Hydrogen atoms have been omitted for clarity.

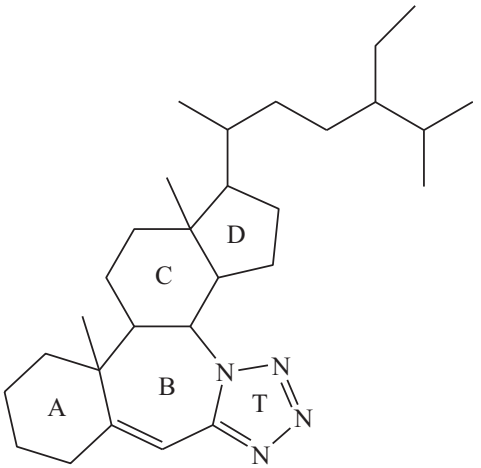

Scheme 2. Assignment of 7a-Aza-B-homostigmast-5-eno [7a,7-d] tetrazole depicting various rings.

Table 2
Cytotoxicity of compound against the cell lines.

Compound	Cell lines		
	HCT116	HepG2	HFL1
7a-Aza-B-homo stigmast-5-eno[7a,7-d]tetrazole	4.58	4.82	Not active
Doxorubicin	2.60	2.85	Not active

The highest concentration tested was 25 μL for compound and all the values are an average of three observations

compounds were compared to doxorubicin (Table 2). The results indicate that the compound inhibits various cancer cell lines in a dose-dependent manner. The antitumor efficacy of the compound may be attributed to its ability to deactivate ribonucleotide reductase, the enzyme that catalyzes the conversion of ribonucleotides to deoxyribonucleotides. As a consequence, the compound interferes with DNA synthesis, thus decreasing the rate of replication of tumour cells and inhibiting tumour growth. The antitumour activity seems to be due to an inhibition of DNA synthesis in cancer cells produced by modification in reductive conversion of ribonucleotides to deoxyribo-nucleotides [25].

3.3. Antimicrobial activity

The antibacterial screening data showed moderate to good inhibition (Tables 3 and 4). The screened compound

Table 3
Antibacterial screening of the compound against Gram positive strains.

S. No	Strain	Zone of inhibition (in mm)		MIC (mg/ml)
		Compound (40 μl/well)	Ciprofloxacin (30 μg/disk)	
1.	*S. aureus*	19	28	0.312
2.	*S. mutans*	25	30	0.078
3.	*S. epidermidis*	23	28	0.078
4.	*S. pyogenes*	30	30	0.078
5.	*B. cereus*	24	30	0.156
6.	*C. xerosis*	27	28	0.078

Table 4
Antibacterial screening of the compound against Gram negative strains.

S. No	Strain	Zone of Inhibition (in mm)		MIC (mg/ml)
		Compound (40 μl/well)	Gentamicin (30 μg/disk)	
1.	*E. coli*	24	27	0.078
2.	*K. pneumoniae*	23	27	0.039
3.	*P. aeruginosa*	24	28	0.078
4.	*P. vulgaris*	25	30	0.019

was found to have good zones of inhibition. The highest activity in case of Gram positive bacteria was observed against *C. xerosi* against the reference drug ciprofloxacin with MIC equal to 0.078 mg/mL. Similarly, the highest activity in the case of Gram negative bacteria was found for *P. vulgaris* in comparison with the standard drug, gentamicin with MIC equal to 0.019 mg/mL.

3.4. Crystallographic studies

An ORTEP drawing with the atomic numbering scheme is shown in Fig. 1 and the crystallographic data, selected bond lengths and bond angles are listed in Tables 5 and 6. It crystallizes in the orthorhombic space group *P212121*. Rings A [with puckering parameters $Q_A = 0.542(6)$, $\varphi_A = 283(6)^\circ$, and $\theta_A = 174.5(6)^\circ$] and C [with puckering

Table 5
Crystal data and structure refinement for 7a-Aza-B-homostigmast-5-eno [7a,7-d] tetrazole.

Compound	7a-Aza-B-homostigmast-5-eno [7a,7-d] tetrazole
Empirical formula	$C_{29}H_{48}N_4$
Formula weight	452.71
Temperature (K)	298(2)
Wavelength (Å)	0.71073
Crystal system	Orthorhombic
Space group	*P212121*
a (Å)	7.230(3)
b (Å)	31.451(13)
c (Å)	11.974(5)
α (°)	90
β (°)	90
γ (°)	90
Volume (Å^3)	2723(2)
Z, ρ_{calc} (g cm^{-3})	4, 1.104
Absorption coefficient (mm^{-1})	0.065
F(000)	1000
Crystal size (mm)	0.40 × 0.34 × 0.30
θ Range for data collection (°)	2.14–25.0°
Limiting indices	$-8 \le h \le 7, -29 \le k \le 37, -14 \le l \le 14$
Reflections collected/unique	14294/4811 [$R_{int} = 0.0912$]
Max. and min. transmission	0.9808 and 0.9745
Refinement method	Full-matrix least-squares on F^2
Data/restraints/parameters	4811/10/298
Goodness-of-fit on F^2	0.917
Final *R* indices [$I > 2\text{sigma}(I)$]	$R_1 = 0.0637$, $wR_2 = 0.1452$[a]
R indices (all data)	$R_1 = 0.1451$, $wR_2 = 0.1813$
Largest diff. peak and hole (e Å^{-3})	0.191 and −0.145
Completeness to $\theta = 25.00$ (%)	99.6
Absolute structure parameter	−3(5)

[a] $R_1 = [\Sigma(|F_o| - |F_c|)]/\Sigma\ |F_o|$; $wR_2 = [\Sigma\ [w(|F_o|^2 - |F_c|^2)^2]/\Sigma\ [w(|F_o|^2)^2]]^{1/2}$; $w = 1/[\sigma^2|F_o|^2 + (x\ p)^2]$; where $p = [|F_o|^2 + 2|F_c|^2]/3$; $x = 0.0605$.

parameters $Q_C = 0.529(4)$, $\varphi_C = 59.3(9)^\circ$, and $\theta_C = 151.7(4)^\circ$] are in their usual chair conformations while ring B is a modified heterocyclic seven-membered ring (B), resulting from the incorporation of tetrazole ring (T) fused to the steroid nucleus. Ring B [with puckering parameters $Q_B = 0.665(4)$] adopts a slightly distorted half-chair conformation as a result of the double bond between atoms C5 and C6. The adjacent bonds C5–C4 and C5–C10 are slightly shorter as a consequence of C5–C6 double bond while C6–C7 has partial double bond character. Consequently, atoms C6 and C8 along with the tetrazole ring form a planar region. The 5-membered ring D is in envelope form at C13. The slight lengthening of the bonds in the chain C(1)–C(10)–C(9)–C(8) linking rings A, B and C is probably due to strain imposed by the additional bond in ring B [26]. The bond distances and bond angles of the compound show a fair amount of agreement with those of some analogous steroids [27–30].

Table 6
Bond lengths [Å] and angles [°] for 2apre.

Bond lengths		Bond angles	
C(1)–C(2)	1.523(6)	N(1)–C(7)–C(6)	121.2(6)
C(1)–C(10)	1.552(5)	C(14)–C(8)–C(9)	115.2(3)
C(2)–C(3)	1.516(6)	C(11)–C(9)–C(10)	110.0(3)
C(3)–C(4)	1.508(8)	C(11)–C(9)–C(8)	113.3(3)
C(4)–C(5)	1.508(7)	C(10)–C(9)–C(8)	114.4(3)
C(5)–C(6)	1.398(6)	C(5)–C(10)–C(9)	116.7(4)
C(5)–C(10)	1.505(6)	C(5)–C(10)–C(1)	105.3(4)
C(6)–C(7)	1.407(7)	C(9)–C(10)–C(1)	107.5(3)
C(7)–N(1)	1.315(6)	C(5)–C(10)–C(19)	105.8(3)
C(7)–N(4)	1.323(5)	C(9)–C(10)–C(19)	112.0(3)
C(8)–N(4)	1.479(4)	C(1)–C(10)–C(19)	109.2(4)
C(8)–C(14)	1.512(5)	C(12)–C(11)–C(9)	118.2(3)
C(8)–C(9)	1.560(5)	C(11)–C(12)–C(13)	111.7(3)
C(9)–C(11)	1.550(4)	N(4)–C(7)–C(6)	129.0(4)
C(9)–C(10)	1.550(5)	N(4)–C(8)–C(14)	108.3(3)
C(10)–C(19)	1.564(5)	N(4)–C(8)–C(9)	107.6(3)
C(11)–C(12)	1.507(5)	C(12)–C(13)–C(17)	117.2(3)
C(12)–C(13)	1.518(5)	C(12)–C(13)–C(14)	105.8(3)
C(13)–C(17)	1.533(5)	C(17)–C(13)–C(14)	100.7(3)
C(13)–C(14)	1.535(5)	C(12)–C(13)–C(18)	110.6(3)
C(13)–C(18)	1.541(5)	C(17)–C(13)–C(18)	109.9(3)
C(14)–C(15)	1.522(5)	C(14)–C(13)–C(18)	112.1(3)
C(15)–C(16)	1.532(6)	C(8)–C(14)–C(15)	117.6(3)
C(16)–C(17)	1.539(6)	C(8)–C(14)–C(13)	114.0(3)
C(17)–C(20)	1.532(5)	C(15)–C(14)–C(13)	104.1(3)
C(20)–C(21)	1.537(6)	C(14)–C(15)–C(16)	104.3(3)
C(20)–C(22)	1.542(5)	C(15)–C(16)–C(17)	107.1(3)
C(22)–C(23)	1.504(6)	C(20)–C(17)–C(13)	119.6(3)
C(23)–C(24)	1.512(7)	C(20)–C(17)–C(16)	111.3(4)
C(24)–C(25)	1.529(7)	C(13)–C(17)–C(16)	103.5(3)
C(24)–C(28)	1.534(6)	C(17)–C(20)–C(21)	113.6(4)
C(26)–C(27)	1.522(5)	C(17)–C(20)–C(22)	109.3(4)
C(27)–C(25)	1.525(7)	C(21)–C(20)–C(22)	109.1(4)
C(29)–C(28)	1.523(5)	C(23)–C(22)–C(20)	118.1(4)
N(1)–N(2)	1.343(5)	C(22)–C(23)–C(24)	116.7(5)
N(2)–N(3)	1.306(5)	C(23)–C(24)–C(25)	111.2(5)
N(3)–N(4)	1.345(5)	C(23)–C(24)–C(28)	111.6(5)
		C(25)–C(24)–C(28)	111.4(6)
Bond angles		C(26)–C(25)–C(27)	113.4(9)
		C(26)–C(25)–C(24)	109.9(6)
C(2)–C(1)–C(10)	116.8(4)	C(27)–C(25)–C(24)	114.6(7)
		C(29)–C(28)–C(24)	119.2(7)
C(3)–C(2)–C(1)	110.6(5)	C(7)–N(1)–N(2)	104.9(5)
C(4)–C(3)–C(2)	108.6(5)	N(3)–N(2)–N(1)	111.6(4)
C(5)–C(4)–C(3)	112.4(5)	N(2)–N(3)–N(4)	105.5(4)
C(6)–C(5)–C(10)	127.1(4)	C(7)–N(4)–N(3)	108.2(4)
C(6)–C(5)–C(4)	115.2(5)	C(7)–N(4)–C(8)	128.0(4)
		N(3)–N(4)–C(8)	123.7(4)
C(10)–C(5)–C(4)	117.6(5)		
C(5)–C(6)–C(7)	130.7(4)		
N(1)–C(7)–N(4)	109.8(5)		

Appendix A. Supplementary data

Crystallographic data for the structural analysis has been deposited with the Cambridge Crystallographic Data Centre, CCDC No. 832006. Copies of this information may be obtained free of charge from The Director, CCDC, 12 Union Road, Cambridge, CB21EZ, UK (fax: +44 1223 336033; e-mail: deposit@ccdc.cam.ac.uk or www.ccdc.cam.ac.uk/data.request/cif).

References

[1] M. Ibrahim-Ouali, et al. Steroids 77 (2012) 1092.
[2] A. Butenandt, G. Hanisch, Z. Physiol. Chem. 237 (1935) 89.
[3] L. Ruzicka, A. Wettstein, H. Kagi, Helv. Chim. Acta. 18 (1935) 1478.
[4] A. Purohit, L.W.L. Woo, S.K. Chander, S.P. Newmana, C. Ireson, Y. Ho, A. Grasso, M.P. Leese, B.V.L. Potter, M.J. Reed, J. Steroid Biochem. Mol. Biol. 86 (2003) 423.
[5] R.N. Bulter, in : A.R. Katrizky, C.W. Rees, E.F.V. Scriven (Eds.), Comprehensive Heterocyclic Chemistry, 4, Pergamon, Oxford, UK, 1996, p. 1.
[6] R.J. Herr, Bioorg. Med. Chem. 10 (2002) 3379.
[7] (a) S. Zhou, Y. Zhou, Y. Xing, N. Wang, L. Cao, Chirality 23 (2011) 504 ; (b) E. Barbayianni, P. Bouzi, V. Constantinou-Kokotou, V. Ragoussis, G. Kokotos, Heterocycles 78 (2009) 1243.
[8] D. Moderhack, J. Prakt. Chem. 340 (1988) 687.
[9] V.A. Ostrovskii, M.S. Pevzner, T.P. Kofmna, M.B. Shcherbinin, I.V. Tselinskii, Targets Heterocycl. Syst. 3 (1999) 467.
[10] (a) Y.H. Joo, J.M. Shreeve, Angew. Chem. Int. Ed. 48 (2009) 564 ; (b) Y.H. Joo, J.M. Shreeve, Angew. Chem. Int. Ed. 49 (2010) 7320 ; (c) D.E. Chavez, M.A. Hiskey, J. Energetic Mater. 17 (1999) 357.
[11] (a) S.K. Figdor, M.S.M. von Wittenau, J. Med. Chem. 10 (1967) 1158 ; (b) C. Rossi, M. Porcelloni, P. D'Andrea, C.I. Fincham, A. Ettorre, S. Mauro, A. Squarcia, M. Bigioni, M. Parlani, F. Nardelli, M. Binaschi, C.A. Maggi, D. Fattori, Bioorg. Med. Chem. Lett. 21 (2011) 2305 ; (c) E.S. Schaffert, G. Hofner, K.T. Wanner, Bioorg. Med. Chem. 19 (2011) 6492.
[12] B.J. Al-Hourani, S.K. Sharma, M. Suresh, F. Wuest, Bioorg. Med. Chem. Lett. 22 (2012) 2235.
[13] T. Jin, S. Kamijo, Y. Yamamoto, Tetrahedron Lett. 45 (2004) 9435.
[14] J. Moural, K. Syhora, Collect. Czech. Chem. Commun. 35 (1970) 2018.
[15] M.S. Ahmad, I.A. Ansari, S.A. Ansari, G. Moinuddine, Indian J. Chem. 24B (1985) 664.
[16] SMART & SAINT Software Reference Manuals, version 6.45; Bruker Analytical Xray Systems, Inc.: Madison, WI, 2003.
[17] G.M. Sheldrick, SADABS, Software for Empirical Absorption Correction Ver. 2.05, University of Göttingen, Germany, 2002.
[18] XPREP, 5.1 ed. Siemens Industrial Automation Inc., Madison, WI, 1995.
[19] International Tables for X-ray Crystallography, vol. IV, Kynoch Press, Birmingham, England, 1974.
[20] G.M. Sheldrick, SHELXL97, Program for Crystal Structure Refinement, University of Göttingen, Germany, 2008.
[21] A.L. Spek, PLATON, A Multipurpose Crystallographic Tool, Utrecht University, Utrecht, The Netherlands, 2005.
[22] L.J. Farrugia, J. Appl. Crystallorg. 30 (1997) 565.
[23] C.F. Macrae, P.R. Edgington, P. McCabe, E. Pidcock, G.P. Shields, R. Taylor, M. Towler, J. vande Streek, J. Appl. Crystallorg. 39 (2006) 453.
[24] P. Bagri, M. Ali, S. Sultana, V. Aeri, J. Asian Nat. Prod. Res. 11 (2009) 710.
[25] S.A.A. Nami, S. Khan, M. Alam, M. Mushfiq, D.-U. Lee, S.H. Park, J. Spect. 28 (2013), http://dx.doi.org/10.1155/2013/128149, Article ID 128149.
[26] J. Husain, R.A. Palmer, H. Singh, T.R. Bhardwaj, D. Paul, Acta Crystallorg. B37 (1981) 205.
[27] Rajnikant, N. Dinesh, M. Aziz, M. Mushfiq, A.U. Alam, Khan, J. Chem. Crystallogr. 36 (2006) 793.
[28] Z. Freixa, M.M. Pereira, J.C. Bayon, A.M.S. Silva, J.A.R. Salvador, A.M. Beja, J.A. Paixao, M. Ramos, Tetrahedron: Asymmetry 12 (2001) 1083.
[29] P. Sharma, P.S. Chauhan, P. Dutt, M. Amina, K.A. Suri, B.D. Gupta, O.P. Suri, K.L. Dhar, D. Sharma, V. Gupta, N.K. Satti, Steroids 76 (2011) 358.
[30] E. Modica, F. Compostella, D. Colombo, F. Ronchetti, A. Scala, B. Bovio, Steroids 68 (2003) 367.